

Direct Observation of Exchange Splittings in Cs₃Tb₂Br₉ by Neutron Spectroscopy

A. Furrer

*Labor für Neutronenstreuung, Eidgenössische Technische Hochschule Zürich,
CH-5303 Würenlingen, Switzerland*

H. U. Güdel

Institut für Anorganische Chemie, Universität Bern, CH-3000 Bern 9, Switzerland

H. Blank and A. Heidemann

Institut Laue-Langevin, 156 X, F-38042 Grenoble CEDEX, France

(Received 23 August 1988)

The inelastic-neutron-scattering technique was used to measure the magnetic excitation spectrum of Tb³⁺ dimers in Cs₃Tb₂Br₉. Between 2 and 3 meV four inelastic transitions are observed which exhibit a different behavior of intensity as a function of momentum transfer. This allows an unambiguous identification of the four types of dimer excitations and, in turn, a direct determination of both the nature and the magnitude of the exchange interaction: It is isotropic with $\mathcal{J} = -0.0049$ meV.

PACS numbers: 71.70.Gm, 75.20.Ck, 75.30.Et

The magnetic properties of compounds containing f electrons result from an interplay of crystalline electric field (CEF) with magnetic dipole and exchange interactions. Experimental data are usually interpreted in terms of an effective Hamiltonian. In extended systems, the empirical parameters thus obtained are often hard to rationalize on a microscopic level due to the cooperative nature of the magnetic effects. This problem can be avoided or greatly reduced by the study of discrete clusters of f -electron ions.

Inelastic neutron scattering (INS) has proved to be a powerful experimental tool for the study of clusters of $3d$ transition-metal ions.¹ In the present Letter we describe the application of the INS technique to the much more complicated case of a $4f$ -electron dimer system. While the determination of CEF interactions by INS experiments is well established today,² the study of the exchange anisotropy in magnetically ordered materials requires a complete measurement of the various branches of the spin-wave spectrum, as well as a suitable model to interpret the experimental data.³ The study of dimers of $4f$ -electron ions overcomes the difficulties that arise with cooperative systems, since the underlying few-body Hamiltonian can be exactly solved. There have been several studies of trivalent lanthanide dimers in doped paramagnetic and diamagnetic host lattices, the main experimental techniques being ESR and magnetic susceptibility measurements.⁴⁻⁶ INS provides the most direct access to the relevant energy splittings and thus a very straightforward determination of exchange parameters.

Cs₃Tb₂Br₉ crystallizes in space group $R\bar{3}c$.⁷ The Tb₂Br₉³⁻ dimers consist of two face-sharing TbBr₆³⁻ octahedra; they have D_3 (approximate D_{3h}) point symmetry, and their threefold axis coincides with the crystal c axis. We neglect interdimer interactions and write the spin Hamiltonian of a Tb³⁺ dimer as follows:

$$\hat{\mathcal{H}} = \hat{\mathcal{H}}_{\text{CEF}}(1) + \hat{\mathcal{H}}_{\text{CEF}}(2) + \hat{\mathcal{H}}_{\text{ex}}(1,2). \quad (1)$$

The first two terms are the usual single-ion Hamiltonians for a trigonal crystal field. They have been given explicitly in Ref. 8. Including anisotropy, the exchange interaction can be expressed as

$$\hat{\mathcal{H}}_{\text{ex}}(1,2) = -2\mathcal{J}\hat{\mathbf{J}}_1 \cdot \hat{\mathbf{J}}_2 - 2\mathcal{J}^z\hat{J}_1^z\hat{J}_2^z. \quad (2)$$

In order to cover the entire range of exchange parameters \mathcal{J} and \mathcal{J}^z , we introduce the following parametrization:

$$\mathcal{J} = Ar, \quad \mathcal{J}^z = A(1 - |r|). \quad (3)$$

A is a scaling factor and r is a measure of the relative magnitudes of \mathcal{J} and \mathcal{J}^z . In this notation we have the Heisenberg model for $r = \pm 1$, the Ising model for $r = 0$, and the XY model for $r = -0.5$.

In an octahedral environment, the CEF ground state of Tb³⁺ is a Γ_1 followed by a Γ_4 . The trigonal symmetry C_3 (approximate C_{3v}) of Tb³⁺ in Cs₃Tb₂Br₉ further splits the cubic Γ_4 triplet into a singlet Γ_2 and a doublet Γ_3 . In order to understand the low-energy excitations of Cs₃Tb₂Br₉, there is no need to consider any higher-lying CEF states.

Eigenvalues of Eq. (1) were obtained as described in Ref. 8; a convenient basis set for this calculation is given by the functions $|J_1J_2JM\rangle$ with $\mathbf{J} = \mathbf{J}_1 + \mathbf{J}_2$. The effect of $\mathcal{H}_{\text{ex}}(1,2)$ on the Γ_1 , Γ_2 , and Γ_3 CEF states for selected values of A and r is illustrated in Fig. 1. The symmetry designation of the dimer states is in D_{3h} . Both \mathcal{J} and \mathcal{J}^z are assumed antiferromagnetic in Fig. 1; for ferromagnetic exchange the dimer states have to be interchanged as follows: $\Gamma_2 \leftrightarrow \Gamma_3$ and $\Gamma_5 \leftrightarrow \Gamma_6$. With our choice of basis the dimer wave functions have the general form

$$|\Gamma_i\rangle = \sum_{J,M} a_i(J_1, J_2, J, M) |J_1J_2JM\rangle. \quad (4)$$

Examination of the wave functions for the relevant dimer states shows that the four transitions from the Γ_1 ground level have different ΔJ and ΔM characteristics as

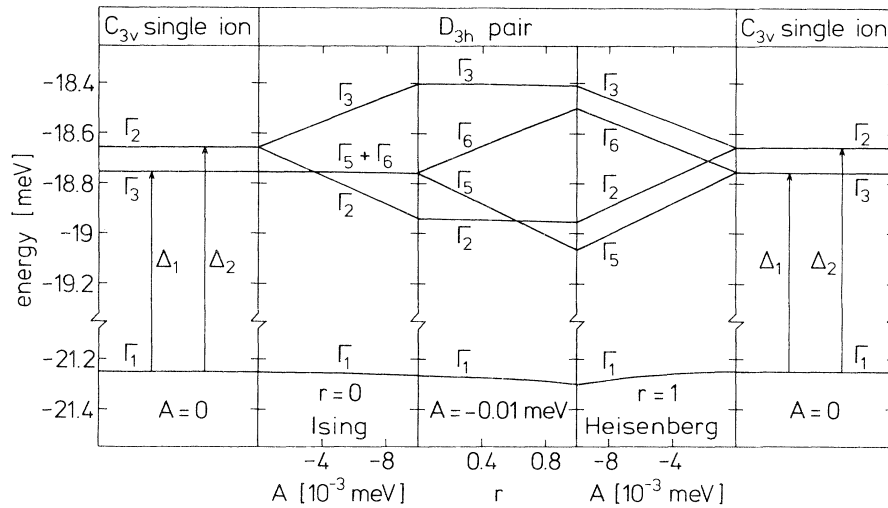


FIG. 1. Exchange-induced splitting of the lowest-energy CEF states of a Tb^{3+} dimer for various values of the exchange parameters A and r expressed in units of the model parameters A and r defined by Eq. (3).

listed in Table I. As elaborated in Refs. 8 and 9, their cross sections for scattering from a polycrystalline sample can be expressed as⁸

$$\frac{d^2\sigma}{d\Omega d\omega} \sim F^2(Q) |\langle \Gamma_i | \hat{T}^{\Delta M} | \Gamma_1 \rangle|^2 I_{\Delta J}^{\Delta M}(Q). \quad (5)$$

$\hat{T}^{\Delta M}$ is an irreducible tensor operator of rank one which is related to \hat{J}_1^{α} and \hat{J}_2^{α} ($\alpha = x, y, z$).⁹ Q is the modulus of the scattering vector, $F(Q)$ is the form factor, and $I_{\Delta J}^{\Delta M}(Q)$ is the so-called interference term,⁹ which clearly discriminates between the four transitions:

$$I_{\Delta J}^0(Q) = \frac{2}{3} + (-1)^{\Delta J} \left[\frac{2 \sin(QR)}{(QR)^3} - \frac{2 \cos(QR)}{(QR)^2} \right], \quad I_{\Delta J}^{\pm 1}(Q) = \frac{2}{3} - (-1)^{\Delta J} \left[\frac{\sin(QR)}{(QR)^3} - \frac{\cos(QR)}{(QR)^2} - \frac{\sin(QR)}{QR} \right], \quad (6)$$

where R denotes the metal-metal distance within the dimer. The four different types of transitions have different Q dependences as shown in Fig. 2.

Literature procedures¹⁰ were used for the synthesis of the polycrystalline compound $\text{Cs}_3\text{Tb}_2\text{Br}_9$ and its diluted analog $\text{Cs}_3\text{Y}_{1.8}\text{Tb}_{0.2}\text{Br}_9$. X-ray and neutron powder diffraction revealed single-phase samples of the expected structure. The INS experiments were performed on the time-of-flight spectrometer IN5 at the high-flux reactor of the Institut Laue-Langevin in Grenoble. The wavelength of the incoming neutrons was varied between 4.8 and 8.0 Å, and the scattering angles covered the range from 2° to 134°. The sample was sealed in a platelike aluminum container of dimensions 45×40×4 mm³ and mounted in a helium cryostat ($T \geq 1.8$ K). The result-

ing time-of-flight spectra were corrected for transmission, detector efficiency, resolution effects, and sample container scattering according to standard procedures.

Experiments on the isostructural diluted compound $\text{Cs}_3\text{Y}_{1.8}\text{Tb}_{0.2}\text{Br}_9$ were used to determine the CEF splittings of Tb^{3+} in this environment. Figure 3 shows the 2-K results at low-energy transfers. Two overlapping bands centered at 2.48 and 2.59 meV which we interpret as $\Gamma_1 \rightarrow \Gamma_3$ and $\Gamma_1 \rightarrow \Gamma_2$ transitions (C_{3v} notation), respectively, are clearly identified. The trigonal CEF splitting of the cubic Γ_4 state is obviously rather small. The effect of exchange coupling is seen in the 2-K spectrum of the undiluted sample $\text{Cs}_3\text{Tb}_2\text{Br}_9$ also shown in Fig. 3. It exhibits two asymmetric peaks around 2.35 and 2.65

TABLE I. Observed and calculated energies (in meV), assignments, and $\Delta J, \Delta M$ characteristics of the four dimer ground-state transitions.

Band	E_{obs}	E_{calc}	$\Gamma_1 \rightarrow \Gamma_i$ (D_{3h} pair notation)	Selection rules
A	2.34 ± 0.02	2.34	$\Gamma_1 \rightarrow \Gamma_5$	$\Delta J = \pm 1, \Delta M = \pm 1$
B	2.43 ± 0.01	2.43	$\Gamma_1 \rightarrow \Gamma_2$	$\Delta J = \pm 1, \Delta M = 0$
C	2.61 ± 0.01	2.61	$\Gamma_1 \rightarrow \Gamma_6$	$\Delta J = 0, \Delta M = \pm 1$
D	2.70 ± 0.01	2.70	$\Gamma_1 \rightarrow \Gamma_3$	$\Delta J = 0, \Delta M = 0$

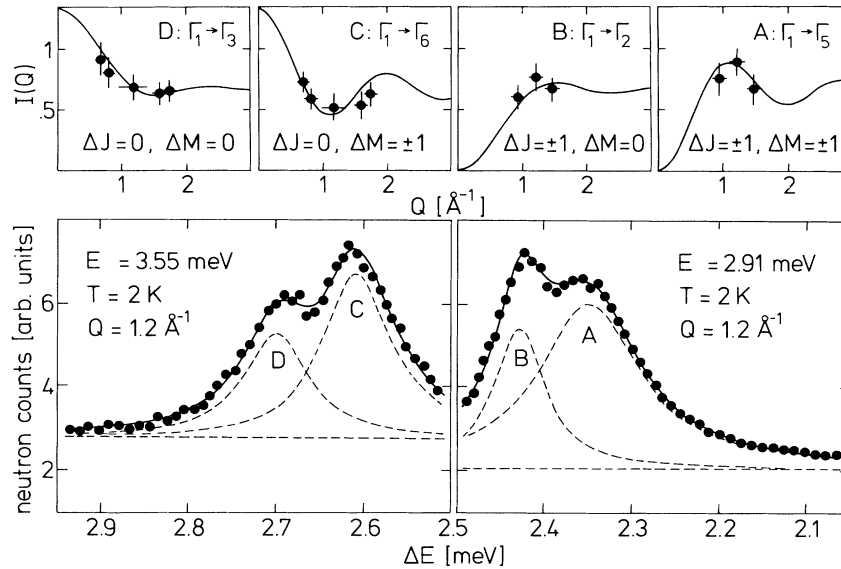


FIG. 2. Energy spectra of neutrons scattered from polycrystalline $\text{Cs}_3\text{Tb}_2\text{Br}_9$. The lines are explained in the text. The top shows the Q dependence of the intensities of the four different dipole transitions defined by Eq. (5). The lines correspond to the interference terms calculated from Eq. (6). The experimental points are the result of a least-squares-fitting procedure described in the text, with corrections due to the form factor and the transition-matrix element [Eq. (5)] taken into account.

meV with different Q dependences. Both peaks are composed of two components, as revealed by the measurements with increased resolution shown in Fig. 2. The Q dependence of all the four transitions could thus be determined by our deconvoluting the overlapping bands as follows. The observed energy spectra were fitted with four Lorentzian lines. A fit with Gaussian-shaped profiles failed to reproduce the pronounced tails and the observed separations of the two

components simultaneously. The net results of the least-squares fits are shown as solid curves in the lower part of Fig. 2; the broken lines indicate the background level and the subdivision into individual transitions. We attribute the rather large width of line *A* to interdimer coupling neglected in our model. As shown in Figs. 2 and 3, both components (*A, B*) of the 2.35-meV peak have a Q dependence typical of $\Delta J = \pm 1$ transitions ($\Gamma_1 \rightarrow \Gamma_2$ and $\Gamma_1 \rightarrow \Gamma_5$ in D_{3h} notation), whereas the components (*C, D*) of the 2.65-meV peak show the opposite behavior, characteristic of $\Delta J = 0$ transitions ($\Gamma_1 \rightarrow \Gamma_3$ and $\Gamma_1 \rightarrow \Gamma_6$). The error bars of the data points on the top of Fig. 2 were obtained from the curve fitting procedure and thus correspond to absolute errors. Consideration of possible systematic errors in our measurements would lead to smaller relative error bars and thus a strengthening of our arguments. In addition to their interference behavior, we used the relative intensities of the four transitions for the assignment. Bands *A* and *C* are approximately twice as intense as bands *B* and *D*, as expected for $\Delta M = \pm 1$ and $\Delta M = 0$ transitions, respectively.

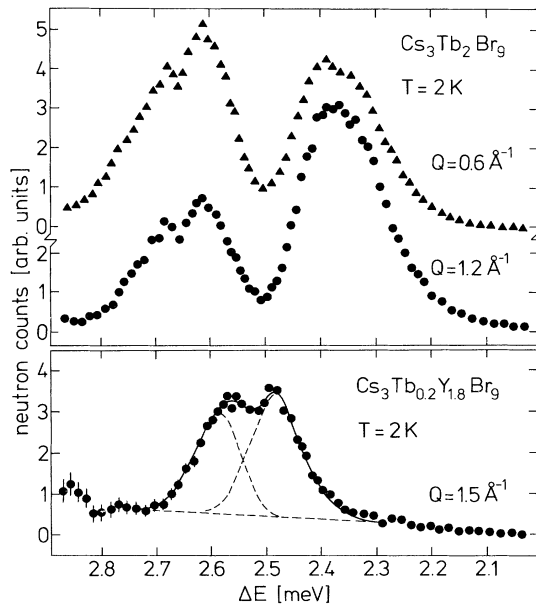


FIG. 3. Energy spectra of neutrons scattered from polycrystalline $\text{Cs}_3\text{Tb}_2\text{Br}_9$ and $\text{Cs}_2\text{Y}_{1.8}\text{Tb}_{0.2}\text{Br}_9$. The energy of the incoming neutrons was 3.55 meV. The curves in the lower spectrum are the result of a least-squares-fitting procedure with Gaussian peak shapes.

Inspection of Fig. 1 reveals that the observed level ordering points to an antiferromagnetic situation with the crystal-field level Γ_3 below Γ_2 . Since the levels *A* and *B* are separated by the same amount as the levels *C* and *D*, the exchange must be isotropic and the following param-

eters are obtained:

$$\Delta_1 = 2.47 \pm 0.01 \text{ meV},$$

$$\Delta_2 = 2.56 \pm 0.01 \text{ meV},$$

$$\mathcal{J} = -0.0049 \pm 0.0004 \text{ meV}.$$

The CEF splittings are very similar to the diluted analog $\text{Cs}_3\text{Y}_{1.8}\text{Tb}_{0.2}\text{Br}_9$, in which Δ_1 and Δ_2 directly correspond to the observed excitations at 2.48 and 2.59 meV, respectively (Fig. 3).

The order of magnitude of the exchange coupling found for $\text{Cs}_3\text{Tb}_2\text{Br}_9$ in this study is in good general agreement with the results obtained for other insulating rare-earth systems.^{4-6,11} In the closely related dimer compounds $\text{Cs}_3\text{Dy}_2\text{Br}_9$ and $\text{Cs}_3\text{Yb}_2\text{Br}_9$ exchange interactions lead to a singlet-triplet splitting of the ground state, which can also be interpreted with an isotropic antiferromagnetic Hamiltonian and \mathcal{J} values of -0.041 and -0.187 meV, respectively.¹² In $\text{Cs}_3\text{Ho}_2\text{Br}_9$, on the other hand, an isotropic exchange Hamiltonian cannot account for the observed energy splittings.¹³ There is, at present, a complete lack of theoretical understanding even of the sign of the exchange parameters.¹¹ Besides the theoretical problems, this is certainly connected with the dearth of reliable experimental data. In the present study we demonstrate the power of the INS technique applied to pure dimer compounds in this area of research. The Q dependence, which clearly discriminates between various types of transitions, removes a great deal of ambiguity in the assignment of experimental peaks. We have used a rather simple effective Hamiltonian, and the nature of the magnetic coupling in $\text{Cs}_3\text{Tb}_2\text{Br}_9$ may be more complicated, with contributions from antisymmetric and higher-order exchange. This does not, however, limit the applicability of the conceptual ideas outlined in the

present Letter. In fact, higher-order exchange terms in S -state systems have only recently become susceptible to experimental observation due to the increased instrumental sophistication of the INS technique.¹⁴

We acknowledge the support of this work by the Swiss National Science Foundation.

¹See, e.g., H. U. Güdel, in *Magneto-Structural Correlations in Exchange-Coupled Systems*, edited by R. D. Willett (Reidel, Amsterdam, 1985), p. 325.

²See, e.g., S. K. Sinha, in *Handbook on the Physics and Chemistry of Rare Earths*, edited by K. A. Gschneider, Jr., and L. Eyring (North-Holland, Amsterdam, 1978), Vol. 1, p. 489.

³See, e.g., B. Hälg and A. Furrer, *Phys. Rev. B* **34**, 6258 (1986).

⁴W. P. Wolf, *J. Phys. (Paris), Colloq.* **32**, C1-26 (1971).

⁵R. L. Cone and W. P. Wolf, *Phys. Rev. B* **17**, 4162 (1978), and references quoted there.

⁶M. Velter-Stefanescu, S. V. Nistor, and V. V. Grecu, *Phys. Rev. B* **34**, 1459 (1986).

⁷G. Meyer, *Z. Anorg. Allg. Chem.* **445**, 140 (1978).

⁸A. Furrer, H. U. Güdel, and J. Darriet, *J. Less-Common Met.* **111**, 223 (1985).

⁹A. Furrer and H. U. Güdel, *Phys. Rev. Lett.* **39**, 657 (1977).

¹⁰G. Meyer, *Inorg. Synth.* **22**, 1 (1983).

¹¹R. W. Cochrane, C. Y. Wu, and W. P. Wolf, *Phys. Rev. B* **8**, 4348 (1973), and references quoted there.

¹²A. Dönni, A. Furrer, H. Blank, A. Heidemann, and H. U. Güdel, *J. Phys. (Paris), Suppl.* (to be published).

¹³A. Furrer and H. U. Güdel, unpublished.

¹⁴U. Falk, A. Furrer, J. K. Kjems, and H. U. Güdel, *Phys. Rev. Lett.* **52**, 1336 (1984), and **56**, 1956 (1986).